

Error Mitigation in Quantum Computers through Instruction Scheduling

Kaitlin N. Smith¹, Gokul Subramanian Ravi¹, Prakash Murali², Jonathan M. Baker¹, Nathan Earnest³, Ali Javadi-Abhari³, and Frederic T. Chong¹

¹University of Chicago

²Princeton University

³IBM Quantum, IBM T. J. Watson Research Center

Abstract—Current quantum devices suffer from the rapid accumulation of error that prevents the storage of quantum information over extended periods. The unintentional coupling of qubits to their environment and each other adds significant noise to computation, and improved methods to combat decoherence are required to boost the performance of quantum algorithms on real machines. While many existing techniques for mitigating error rely on adding extra gates to the circuit [12], [39] or calibrating new gates [35], our technique leverages the gates already present in a quantum program and does not extend circuit runtime duration. In this paper, we exploit scheduling time for single-qubit gates that occur in idle windows, scheduling the gates such that their timing can counteract some errors.

Spin-echo corrections act as inspiration for this technique, which can mitigate dephasing, or phase accumulation, that appears as a result of qubit inactivity. Theoretical models, however, fail to capture all sources of noise in near-term quantum devices, making practical solutions necessary that better minimize the impact of unpredictable errors in quantum machines. This paper presents TimeStitch: a novel framework that pinpoints the optimum execution schedules for single-qubit gates within quantum circuits. TimeStitch, implemented as a compilation pass, leverages the reversible nature of quantum computation to improve the success of quantum circuits on real quantum machines. Unlike past approaches that apply reversibility properties to improve quantum circuit execution, TimeStitch boosts fidelity without violating critical path frontiers in either the slack tuning procedures or the final rescheduled circuit. On average, TimeStitch is able to achieve 24% improvement in success rates, with a maximum of 75%, while observing depth criteria.

I. INTRODUCTION

Quantum computing is a revolutionary computational model that leverages quantum mechanical phenomena for solving intractable problems. Quantum computers (QCs) evaluate quantum circuits, or programs, in a manner similar to classical computers, but quantum information’s ability to leverage superposition, interference, and entanglement is projected to provide QCs significant advantage in cryptography [32], chemistry [16], optimization [20], and machine learning [5] applications.

The noisy quantum computing era is defined by QCs available in the near-term that are less than 1000 qubits in size that do not implement fault-tolerant error correcting

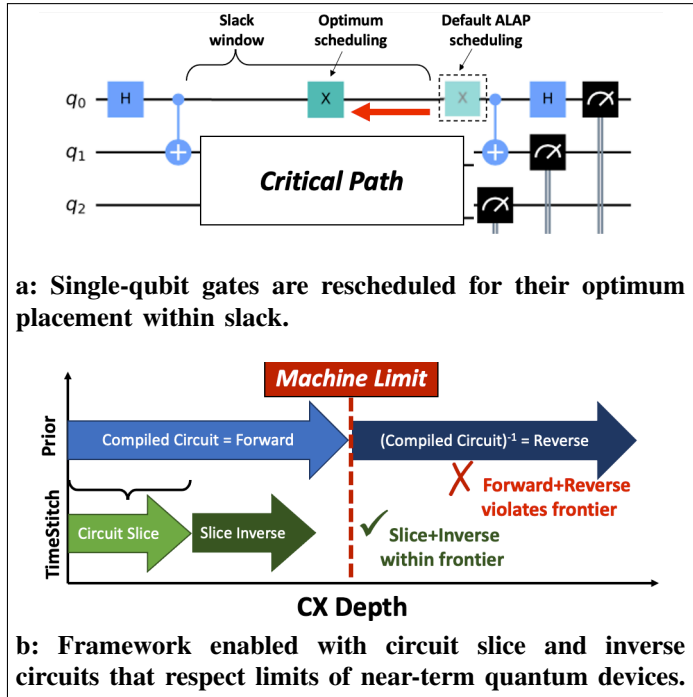


Fig. 1: Overview of the TimeStitch proposal

codes [27]. These devices suffer from high error rates as noise is introduced during state initialization, gate application, and measurement procedures. In addition to errors during operations, qubits also vulnerable to errors during periods of inactivity. These errors are termed *decoherence* i.e., the quality of their state degrades exponentially with time, and manifests in terms of amplitude and phase damping errors. Several near-term applications include large periods of qubit inactivity and hence, they are prone to high decoherence errors.

State-of-the-art decoherence mitigation techniques usually suffer from increased gate counts [39] which can themselves be critically detrimental to circuit fidelity on near-term quantum hardware. Thus, our work aims at decoherence mitigation without additional gates. We present a novel technique to optimize circuits by taking advantage of flexible scheduling within *slack windows*, or periods where a qubit idles as it

waits for its next operation. The benefits of our approach are achieved without extending circuit runtime through either increasing total gate count or introducing circuit partitioning.

Scheduling slack may appear to be a minor component in unmapped circuits, but the impact and duration of idling qubits becomes obvious post compilation. A number of emerging QC technologies, such as superconducting circuits, feature nearest-neighbor topologies with sparse connectivity across qubits. However, important QC applications have communication requirements that do not align well with hardware capabilities. As a result, routing via *SWAP* networks is required for intra-chip qubit communication. These *SWAP* networks increase the duration of quantum circuits, forcing a significant portion of physical qubit runtime, or time from state initialization until final measurement, to be suspended within slack.

Typical circuit scheduling methods such as as late as possible (ALAP) scheduling (a default approach in IBM Qiskit [4]) assume that single-qubit operations are best placed at slack window boundaries. An example of ALAP scheduling is pictured in Fig. 1(a) as an X gate in a dashed box. Our proposal reschedules single-qubit gates potentially away from their ALAP default positions to optimum placements *within circuit slack*, also shown in Fig. 1(a). The chosen gate position is deemed optimum by measuring the fidelity impact of each potential gate position (in its slack window) on a carefully designed tuning circuit. The tuning circuit and its gate position tuning involve slicing the original circuit up to a target slack window and then intelligently leveraging the reversible nature of quantum computing, and is thus referred to as a “Slice + Inverse” approach.

Critical to the near-term, our technique exploits reversibility without exceeding the machine fidelity limits on circuit depth. Prior work exploiting reversibility for predicting circuit outcomes [24] builds a concatenated forward+reverse of a quantum circuit in its entirety, resulting in double the depth of the original circuit. Under the reasonable assumption that target circuits are already at (or just under) the limit of machine capability in terms of circuit depth (which is almost always the goal on near-term QCs), this means that the depth of such concatenated forward+reverse circuits can far exceed the machine’s limits on circuit depth. This is shown in Fig. 1(b) in blue. Section II-B discusses prior work in greater detail. On the other hand, our proposal is constrained to specifically target slack windows whose corresponding SI circuits (slice + inverse) are within the machine limits of circuit depth. This is shown in green in Fig. 1(b). Further, we show that even with this constraint we are able to reap most of the potential benefit from our decoherence mitigation approach - because it still allows us to target most larger slack windows which a) have higher potential for gate position tuning based benefits and b) create circuit slices of lower gate depth due to the very definition of slack.

Fig. 2 depicts a quantum compilation flow that includes the TimeStitch (TS) slack optimizing scheduler which consists of two components. The first component is a module that identifies slack windows within a compiled quantum program

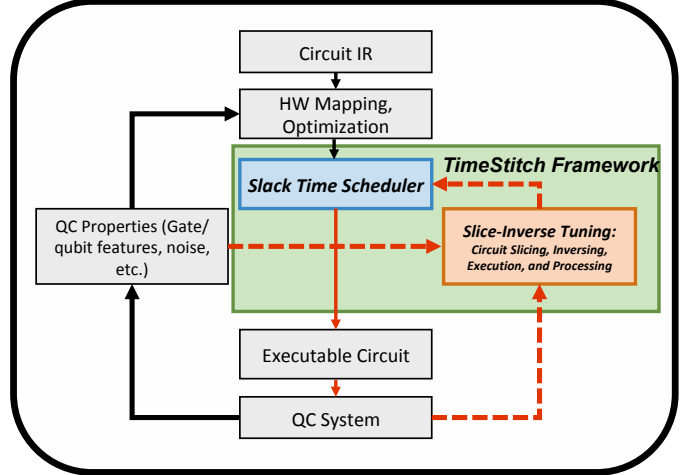


Fig. 2: QC compilation integrated with TimeStitch.

and develops slack tuning circuits through circuit slicing and inversion procedures. These circuits are then used to independently optimize single-qubit gate positions within individual slack windows. Compilations and device properties are subject to variation, thus the optimum placements determined by slack tuning will be unique for each circuit at a given period of time. After finding the optimum scheduling data, the TimeStitch slack time scheduler creates a final “stitched” executable that is an optimized form of the original compiled circuit.

Finally, the fundamental theme of exploiting slack in quantum circuits has significant parallels to slack-based optimization in classical computing, such as those at the circuit-level as well as the microarchitecture-level; we dive deeper into these parallels in Section VII.

Contributions:

① We observe the creation of slack windows as a result of compilation and identify their potential for quantum circuit optimization.

② We design and implement a slack analysis and circuit construction method that analyzes compiled quantum circuits, identifies slack windows, and “slices” the original circuit to isolate dependency graphs up until instances of slack. These “slices” are then combined with a delay line equal to the corresponding slack window followed by the slice inverse circuit to create a total circuit that evaluates to the input state of the slice.

③ We design and implement the TimeStitch Slice-Inverse (TS-SI) slack time scheduler that optimizes the scheduling of single qubit gates within slack. Local optimals are learned during tuning procedures when individual slack windows are searched within slice-inverse circuits to maximize the fidelity of the known ground truth. TS-SI then “stitches” a final quantum circuit with optimum placements identified from tuning. During tuning procedures and final circuit creation, the bounds of the original circuit depth are respected as criteria for tuning (TS-SI+C).

④ We design and implement an ideal ground truth based

“search and stitch” scheduler, TimeStitch Ground Truth (TS-GT), that finds the ideal schedule for a quantum circuit using the quantum circuit directly via exploring each slack window independently and creating a final circuit that stitches together all optimum placements. This approach requires knowledge of a circuit’s true output.

⑤ We compare a variety of benchmark circuits transformed by baseline compilation, TimeStitch Slice-Inverse rescheduling and TimeStitch Ground Truth rescheduling and provide analysis.

⑥ Finally, we implement TimeStitch to suit deployment on real quantum machines and offer insights that can improve the realistic design of future quantum optimization proposals.

Impact:

To our knowledge, this is the first proposal to exploit optimum scheduling of quantum operators within slack windows.

While many existing techniques for mitigating error rely on adding extra gates to the circuit [12], [39] or calibrating new gates [35], TimeStitch leverages the gates already present in a quantum program.

A novel aspect of our framework is that unlike previous proposals that employ reversibility through “forward” and “reverse” circuits [24], program duration is not extended either during tuning procedures or in the final rescheduled output circuit. This is critical in the near-term wherein machines are aggressively utilized at the highest limits of circuit fidelity.

II. BACKGROUND

A. Quantum Information and Technology

The basic unit of quantum information is the quantum bit, or qubit, which can exist in a linear superposition of basis states $|0\rangle$ and $|1\rangle$. If measured, however, the state $|\psi\rangle = \alpha|0\rangle + \beta|1\rangle$ collapses into either $|0\rangle$ or $|1\rangle$, effectively becoming a classical bit. A system of n qubits requires 2^n amplitudes to describe the state.

Qubits are manipulated via gates, unitary and therefore reversible operators, which modify the amplitudes. Quantum operations always have the same number of inputs as outputs. Unlike in classical computation, there are many non-trivial one qubit gates such as $R_x(\theta)$ and $R_z(\theta)$ which rotate the state around the x and z axes, respectively. Pairs of qubits can be manipulated via multi-qubit interactions. The most common of these gates is the CX . Together with single qubit gates, CX enables universal quantum computation. There are many choices of basis gate sets specified by the underlying hardware. For more information on the fundamentals of quantum computation we refer to [23].

Most quantum algorithms are expressed in the circuit model which is simply an ordered list of instructions. A very simple example is found in Figure 1(a) where time flows from left to right and each line represents a single qubit. Gates operate on one or more qubits and measurement is represented as meters at the end of computation. Most available hardware only supports single and two qubit gates and any other more complex gate must first be decomposed into these types

of gates. Current hardware has limited connectivity between qubits and gates may only be performed between qubits which are adjacent on hardware. If logical qubits must be interacted but are distant, communication operations, often in the form of *SWAPs*, are inserted into the program to move them close on the device. All quantum operations are reversible (except measurement) and therefore any circuit has a corresponding inverse circuit which will “undo” the computation of the original circuit.

Current QCs, sometimes called Noisy Intermediate Scale Quantum (NISQ) devices, are error prone and less than 100 qubits in size [27]. These devices are extremely fragile, and as a result, some of the biggest challenges that limit scalability include limited coherence, gate errors, readout errors, and connectivity. Systematic error is restrictive, but once the error is identified it can be effectively mitigated or corrected for in software. The two primary causes of loss of performance are decoherence and crosstalk.

The source of many errors in quantum systems is interaction with the environment. For example, amplitude dampening describes the sporadic loss of energy resulting in the $|1\rangle$ state falling to the $|0\rangle$ state; the rate of this process is described by the device’s T_1 time. Similarly dephasing details the sporadic change in relative phase and is expressed by the T_2 time of the device. Both are the cause of decoherence. Finally, crosstalk refers to error caused by simultaneous execution of gates on nearby qubits. The severity of each of these types of noise varies per qubit and calibration cycle.

B. Considerations with Applied Reversibility

Quantum computation demonstrates the property of reversibility; quantum operations are unitary. A requirement for a unitary operation, U , is that $UU^{-1} = U^{-1}U = I$ where U^{-1} is the operation inverse and I is the identity operation that produces an output equal to the input. As a note, measurement of a quantum circuit is not reversible as it collapses superimposed qubits into a classical bitstring.

A quantum circuit followed by its logical inverse, or “reverse,” produces a known quantum state as the output of the combined “forward+reverse” equals the input. In QRAFT [24], quantum reversibility is effectively applied to reduce error in circuits by increasing the likelihood of determining the correct evaluation output. Since the true output is known for forward+reverse characterization circuits, generated characterization data trains a machine learning model to discern noise attributes of the selected QC. Next, the model is used to predict true outcomes of quantum circuits in their forward+reverse form. While [24] provides a boost in quantum circuit accuracy, it assumes the ability to successfully run quantum algorithms where critical paths, or depths, are twice that of the original circuit. While this may be a reasonable approach for small quantum circuits that terminate well within coherence times, computational hardware is ideally maximized in practical applications. As a result, circuits operating at the boundary of machine thresholds may not produce reliable results if executed in their forward+reverse form. To avoid observing

an output that resembles a random distribution, optimizers invoking reversibility should consider the duration of the original quantum circuit as bounding criteria that should not be violated.

In this work, quantum reversibility is leveraged by TimeStitch to enable the optimization of single-qubit placement within slack. Unlike [24] that applies reversibility towards predictive models, we utilize the true output provided by inverting a quantum circuit to produce circuit schedules that outperform baseline ALAP compilations. These improvements are achieved without exceeding the critical path criteria either during slack tuning or in the final produced circuit. A full description of the TimeStitch framework is found in Section IV with details about circuit depth constraints specifically found in section IV-D.

III. THEORY FOR SLACK WINDOW OPTIMIZATION

A. Qubit Idling in Compiled Circuits

We define qubit runtime as the period spanning the first application of a gate up until measurement. During its runtime, a qubit will spend some cycles within computation and others idle while waiting for signals to propagate along a critical path. Idle time is referred to as slack.

Limited connectivity associated with many quantum technologies requires *SWAP* networks in mapped circuits for qubit communication. Logically, communication constraints of nearest-neighbor QCs will cause an increase in circuit slack as algorithms scale in number of qubits. By default, compilation tools tend to schedule single-qubit operations within slack windows for as late as possible (ALAP) meaning that gates will not execute until another operation, typically either a measurement or a two-qubit operation along a critical path, can be executed immediately afterwards. Scheduling qubit operations for ALAP assists with mitigating noise associated with T_1 and T_2 decoherence if qubit runtime has not initialized. ALAP execution, however, is not always ideal once a qubit holds state as it is more vulnerable to decoherence. Rather than tolerate slack as an unavoidable artifact of compilation and assume ALAP gate defaults, we are motivated to explore both theoretical and practical techniques for the mitigation of phase accumulation within them.

B. Phase Accumulation

To preserve quantum state without corrective codes, open-loop error mitigation procedures can be applied to refocus signals. An example of this type of correction is dynamical decoupling (DD) [39] that “decouples” compute qubits from noise introduced from the environment. The most elementary form of DD suppresses single-qubit phase accumulation with Hahn spin-echo techniques where $R_x(\pi) = X$ instructions are inserted into circuits during runtime. These instructions reverse the impact that dephasing has on quantum state over time. For example, consider a quantum state $|\psi\rangle = \frac{|0\rangle + i|1\rangle}{\sqrt{2}}$. This qubit that sits on the positive y-axis of the Bloch sphere is pictured in Fig. 3(a). In an ideal system, $|\psi\rangle$ would hold state information for infinite time, but phase information is highly

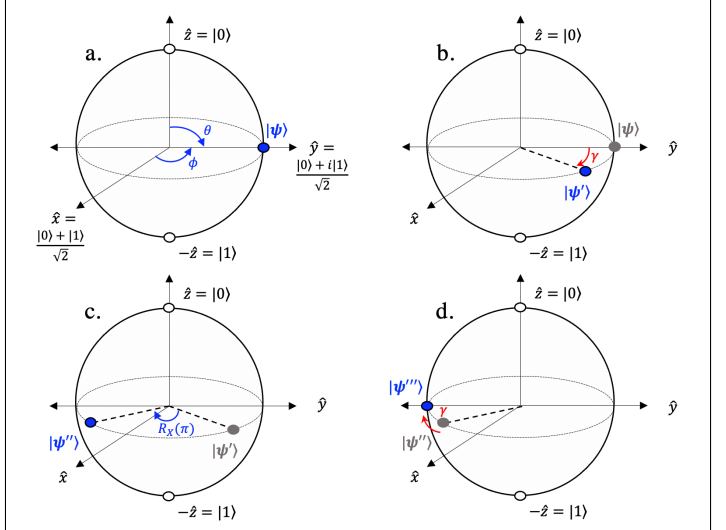


Fig. 3: Phase accumulation mitigation through Hahn spin-echo techniques. (a) A qubit $|\psi\rangle$ rests on the y-axis of the Bloch sphere. (b) As time elapses, the phase state $|\psi\rangle$ decays, and noise in the form of $R_z(\gamma)$ creates the quantum state $|\psi'\rangle$. (c) A $R_x(\pi)$ is applied to the qubit to produce $|\psi''\rangle$, and (d) the effects of dephasing begin to constructively interfere with $|\psi''\rangle$ to produce the phase-coherent state $|\psi'''\rangle$. Another $R_x(\pi)$ pulse restores $|\psi\rangle$ from $|\psi'''\rangle$.

susceptible to decoherence. In Fig. 3(b), the decay of state information is represented by the unknown rotation $R_z(\gamma)$ that causes $|\psi\rangle$ to evolve to $|\psi'\rangle$. Hahn spin-echo techniques apply a $R_x(\pi)$ operation to $|\psi'\rangle$ in Fig. 3(c) to mitigate the phase accumulation caused by decoherence. State $|\psi''\rangle$ results from the flip of $|\psi'\rangle$ across the x-axis. The continued dephasing shown in Fig. 3(d) counteracts the original rotation of $R_z(\gamma)$, refocusing phase information to produce qubit $|\psi'''\rangle$. Restoring the original state $|\psi\rangle$, pictured in Fig. 3(a) with phase information intact, is possible with the application of a final $R_x(\pi)$ pulse to $|\psi'''\rangle$. The procedure of inserting $R_x(\pi)R_x(\pi) = XX$ mid-circuit preserves the semantics of the original circuit as the X operation is self-inverse and $UU^{-1} = I$ where I is the identity operation that does not evolve qubit state. The XX sequence implements the most basic form of DD that provides Hahn spin-echo corrections. Standard DD with the “universal decoupling” sequence requires four gates: $R_x(\pi)R_y(\pi)R_x(\pi)R_y(\pi) = XYXY$ [39].

The circuit in Fig. 4(a) demonstrates the severity of T_2 dephasing. This circuit, referred to as *H + Delay*, consists of a *H* gate followed by a varied delay created by inserting the *I* operation from 0 to 799 times. When evaluated on an QC, the *H* gate initializes a qubit to a superposition of $|\psi\rangle = \frac{|0\rangle + |1\rangle}{\sqrt{2}}$, so that the theoretical probability of measuring either $|0\rangle$ or $|1\rangle$ is 50%. In an ideal quantum system, this probability distribution would stay constant, regardless of the amount of delay until measurement. Actual quantum systems,

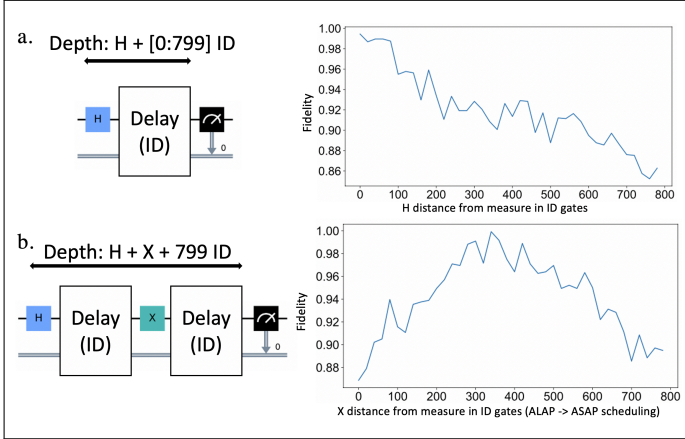


Fig. 4: Demonstration of dephasing over time and potential for correction via Hahn spin-echo techniques. (a) $H + \text{Delay}$ shows lower Hellinger fidelity between experimental results and an ideal balanced superposition as the delay before measurement increases. (b) $H + X + \text{Delay}$ reveals the output distribution approaches theoretical results when X is closer to the middle of the slack window.

unfortunately, do not maintain coherence for extended periods of time. The case study in Fig. 4(a) shows that the $H + \text{Delay}$ circuit has a higher probability of decohering and demonstrates lower Hellinger fidelity between experimental results and an ideal balanced superposition as the delay before measurement increases. Fig. 4(b) explains how Hahn spin-echo correction combats dephasing errors appearing in the Fig. 4(a) test. The circuit of Fig. 4(b) is referred to as $H + X + \text{Delay}$, and it includes an H gate, an X gate, and a total of 799 I gates that are distributed between two delay windows on either side of the X gate that can range from 0 to 799 I gates in size. This test simulates tuning an X gate within a circuit slack window. For this test, circuits were generated that allow the X gate to sweep various schedules within the slack ranging from an ALAP schedule with X placement immediately before the measurement gate to an as soon as possible (ASAP) schedule immediately after the H gate. Evaluation on a QC confirmed that scheduling the X gate approximately midway through the delay window produces an output distribution that closely matches ideal simulation. These results motivate the correction of dephasing through improved scheduling of single-qubit gates within slack.

In realistic workloads, many variables exist such as variation of the rotation angle of the single-qubit gate, the qubit that the gate acts on, the slack window state, and the slack duration. The theory alone does not provide a clear prediction of optimum schedule for general use cases, motivating the need for solutions that rely on empirical observations, which we pursue by exploiting the quantum property of reversibility.

C. Understanding Real-machine Impact

1) *Crosstalk*: Crosstalk is the accidental transfer of a qubit's information to its surrounding qubits. Two adjacent

gates, especially two-qubit interactions, executed simultaneously and within close proximity on a nearest-neighbor QC often demonstrate a lower gate fidelity as a result of crosstalk. Because of the severity of crosstalk, software mitigation techniques have been proposed [8], [22].

It is known that single-qubit, single-qubit crosstalk is trivial [22]. Thus, the scheduling of single-qubit gates in adjacent slack windows can be tuned independent of one another. Discussion our framework's slack tuning procedures is found in Section IV.

2) *Variation in Qubit Characteristics*: Near-term quantum machines are affected by non-deterministic spatial and temporal variations in their characteristics, for instance, in terms of their one- and two-qubit error rates. Prior work [34] observed the prevalence of a wide distribution of machine characteristics with considerable spatial and temporal variation. From the spatial perspective, they observe the coefficient of variation to be in the range of 30-40% for T_1/T_2 coherence times, as well as nearly 75% for 2-qubit error rates. From a temporal perspective, they observe more than 2x variation in error rates in terms of day-to-day averages.

3) *State Diversity within Slack Windows*: Each quantum algorithm has a unique objective, resulting in a large amount of state variation during computation, especially within slack. As previously mentioned, every QC has a distinct noise signature, and this will impact an idling qubit with varying severity depending on its state value. It should also be noted that certain states are more vulnerable to error. For instance, $|1\rangle$ is more vulnerable to T_1 amplitude dampening than $|0\rangle$, and T_2 dephasing caused by phase accumulation is highly influential to superimposed states such as $\frac{|0\rangle+|1\rangle}{\sqrt{2}}$.

Because of variation within quantum machines (III-C2) and circuits (III-C3), it is challenging to develop an umbrella benchmark (or a set of benchmarks) for slack tuning that accurately captures unknown state and error attributes seen in real QC execution. Thus, we are motivated to use the circuits and the machines under investigation themselves, building upon the reversible nature of quantum computation, as the basis for slack tuning to capture state diversity while searching for optimum single-qubit execution schedules.

IV. DESIGNING THE TIMESTITCH FRAMEWORK

In this section, we discuss the design of the TimeStitch framework for slack window gate optimization in real quantum machines. In Section IV-A, we highlight the theoretical lessons learned from Section III that aid in building a design for optimally scheduling gates in slack windows. Then in Section IV-B we propose an *ideal* implementation for gate scheduling. The ideal framework, while providing maximum benefits, is unrealistic as a practical implementation (except for specific usecases) and hence predominantly serves to validate our results from the practical approach. Next, in Section IV-C, we detail our practical proposed framework, built atop theoretical foundations. In this section the practical framework is unconstrained in terms of circuit depth and is potentially suited to low-depth circuits. Finally in Section IV-D we restrict

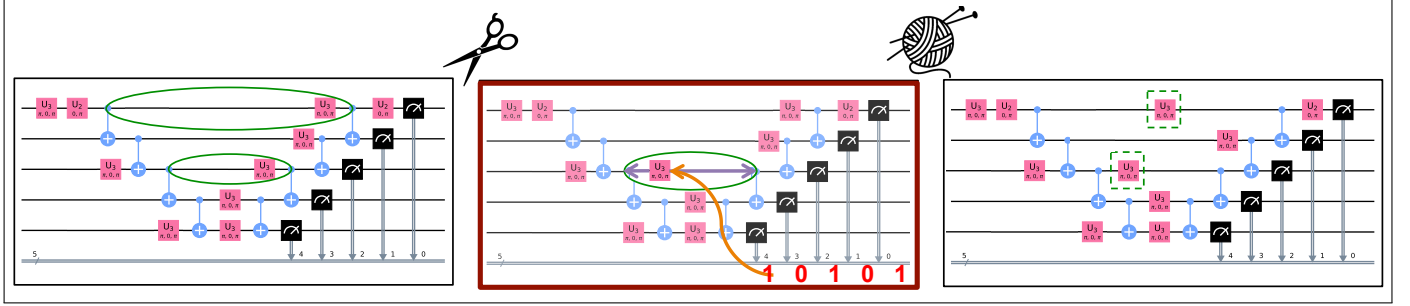


Fig. 5: “Ground Truth” approach framework overview - (Left:) Circuit is compiled to the target machine and slack windows for tuning are identified throughout the quantum circuit. (Middle:) Gate position in each slack window is tuned independently to maximize overall application fidelity - this uses the ground truths or known application outcomes. (Right:) Tuned gate positions are stitched together to construct an optimized circuit schedule.

the above framework to the depth of the original application, thus are compliant with real-world constraints in improving the fidelity of hard-to-execute applications which are the critical circuits for quantum optimization.

A. Lessons from the Theory

For slack optimization, our proposal for a practical approach is built on the following theoretical lessons:

① Slack windows exist in device-mapped quantum circuits, and their amount and duration are correlated to the size of quantum circuit.

② Opportunities for improving the fidelity of quantum circuits exist through adjusting the execution of single-qubit gates from ALAP scheduling to earlier placement within slack windows.

③ Minimal impact of single-qubit crosstalk means that the single-qubit gate position in each slack window can be optimally tuned independent of those in other slack windows.

④ The dependency of gate position within a slack window on gate / qubit characteristics as well as the input state to the slack window, means that offline machine characterization on test inputs and circuits is insufficient / impractical for finding optimal gate positions.

B. An Ideal “Ground Truth” Approach

In this section, we propose an ideal approach for tuning gate positions within slack windows. This approach is ideal because it utilizes the successful circuit outcome (i.e. ground truth) to tune the gate to the optimal position within the slack window. An overview of the framework is shown in Fig. 5 and is discussed below.

1) *Baseline Compilation of the Quantum Circuit:* The TimeStitch framework begins with a quantum circuit compiled from a device-independent intermediate representation (IR) into machine-ready code. Baseline methodology is discussed in Section V-C. The compiled circuit is as shown in the left circuit of Fig. 5.

2) *Identifying Slack Windows:* The TimeStitch framework identifies quantum circuit slack windows after baseline compilation into a QC executable. The identification procedure

requires traversing the components of a quantum circuit that implements default ALAP scheduling from end to end. During this procedure, slack windows are found, and their durations are calculated using gate timing data collected from the QC. A subset of windows are identified that contain single-qubit operators eligible for rescheduling within slack. Two such windows are circled in green in the left circuit of Fig. 5. As a note, we do not consider the time before the first operation on a qubit as slack as the qubit is uninitialized and qubit runtime has not begun.

3) *Optimal Gate Placement in Slack Windows (GT):* After the slack windows are identified, each window is tuned individually for optimum placement while all other windows are held at a default ALAP schedule. The tuning is performed by sweeping the gate position over the slack window and identifying the positions where the fidelity is maximized. Note that to know if fidelity is maximized, this approach uses knowledge of the correct circuit outcome i.e. the ground truth. The fidelity itself is estimated by executing the tuning circuits on the quantum machine. This is shown in the center circuit in Fig. 5 wherein the gate position in the slack window in green is tuned so that the probability of the circuit achieving the application’s ground truth $|10101\rangle$ (shown in red) is maximized.

Note that the resolution of the gate position sweep are constrained by the available resources in the quantum execution framework (discussed further in Section V).

4) *Stitching the Per-window Positions Together:* After the optimal schedules (i.e. gate position in the slack window) are estimated, schedules are stitched together to form a composite, rescheduled circuit. The stitched circuit is pictured in the right of Fig. 5.

5) *Framework Utility:* As discussed above, this approach utilizes the circuit’s ground truth to identify the optimum gate position within slack windows. This is unrealistic for general quantum circuits wherein the successful circuit outcome is unknown prior to quantum execution and is not even necessarily the outcome with highest outcome probability. Thus in the general scenario, this ground truth approach is only suitable as a validation or optimal performance target for a more practical

approach.

In the specific case of state preparation circuits for other quantum circuits, the ground truth approach has practicality. These quantum circuits target the preparation of a particular quantum state (i.e. a known target outcome), and thus their gate schedules can be optimized based on the knowledge of the ground truth. Examples of prepared states are the GHZ and the Gibbs states which are discussed in Section V-B.

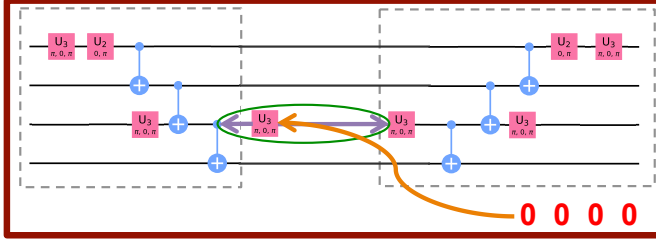


Fig. 6: The key “Slice + Inverse” step that replaces the middle stage in Fig. 5. In the absence of known circuit outcomes, gate positions are optimized by exploiting circuit reversibility. For each slack window, a circuit slice from circuit start to the slack boundary is constructed and concatenated with its inverse. The gate position in the target window is tuned within this circuit, with the goal to make circuit output match the inputs ($|00\dots0\rangle$), implying position of maximum fidelity.

C. A Practical “Slice + Inverse” Approach

In this section we propose the practical approach for gate position optimization within slack windows. At its core, the practical approach leverages the quantum phenomenon of reversibility to adjust the execution timing for single-qubit gates within slack windows - through the process of circuit slicing and inverting (SI). The specific difference in the TimeStitch-SI framework compared to the Ground Truth framework is in the construction of the SI based tuning circuit. This is illustrated in Fig. 6 and is discussed in detail in the rest of this section.

1) *Compilation and Identifying Slack:* These steps are identical to those in the Ground Truth approach discussed in Section IV-B1 and IV-B2. They can be referred to in the left of Fig. 5.

2) *Generation of Slice-Inverse Calibration Circuits:* In the absence of the circuit ground truth (as is commonly applicable to most quantum circuits), tuning is more challenging compared to the earlier approach. This is the key different step in comparison to the Ground Truth approach. The challenges and approach chosen are described here:

① We restate that our goal is to find the optimum gate position within each slack window such that the fidelity of the circuit is maximized - these would be the same slack windows circled in Fig. 5.

② Localizing our goal to a particular slack window (say the window circled in green in Fig. 6), the target is to maximize the fidelity of the circuit state produced at the end (i.e. output) of this slack window. Maximizing the fidelity at this slack

window would improve fidelity overall circuit. (Note: Fig. 6 only replaces the middle circuit from Fig. 5 boxed in brown.)

③ We employ the property of quantum circuit reversibility to maximize the fidelity at the end of this slack window. The concept of reversibility was described in Section II-B.

④ A circuit slice is constructed for each target slack window, ending at the end point of the particular window. Implementation-wise this circuit slice is a subcircuit of the original circuit consisting of the dependency graph up until end of the slack window. Thus the output of the circuit slice emulates the activity of the circuit at the end-point of the window.

⑤ The inverse of the circuit slice is then constructed and concatenated at the endpoint of the slice. The slice + inverse (for this particular slack window) is shown in dashed boxes in Fig. 6 and is called a Slice + Inverse (SI) circuit. Measurement operations complete the SI circuit (not shown).

⑥ In an ideal noise-free setting, the concatenation of a slice and inverse would produce the slice’s input as the output at the end of the inverse because of reversibility.

⑦ In a realistic noisy setting, our goal is then transformed to optimize the gate position in the slack window so that the probability of achieving the slice input state as the output of the concatenated circuit is maximized. This is equivalent to maximizing the circuit fidelity of the original slice (under the reasonable assumption that noise impact on the slice and its inverse are correlated).

⑧ The input state to the slice is trivially known if the slice is constructed from the start of the entire quantum circuit - it is the ground state or $|00\dots0\rangle$. Then the target output of the SI is also $|00\dots0\rangle$ (i.e. it collapses back to ground state) as shown in red in Fig.6.

⑨ Since input states, gates and noise characteristics all influence the optimal gate position, each slack window has to be sliced individually and unique SI circuits are constructed in an automated manner. The total number of SI tuning circuits for an input circuit is equal to the number of identified slack windows with single-qubit operations in the circuit.

⑩ Note that the maximum depth of an SI would be approximately twice the depth of the original circuit (if a slice extends close a circuit’s completion). In the approach discussed in this section, we do not limit the depth of the SIs - constraining the depth is motivated and discussed in Section IV-D.

3) *Optimal Gate Placement in Slack Windows (SI):* Performing the tuning for optimal gate placement within the slack windows is similar to the Ground Truth approach (Section IV-B3) except that the tuning is performed on the slack windows of the SI circuits described above (with $|00\dots0\rangle$ as the target outcome) instead of the original circuit utilized by the ground truth approach.

4) *Stitching the Per-window Positions Together:* The final stitching step is identical to that described in the TS Ground Truth approach in Section IV-B4 and can be referred to in the rightmost circuit of Fig. 5.

D. Constraining by Circuit Depth

The total number of SI tuning circuits is equal to the number of slack instances that contain tunable single-qubit gates. However, some of these SI circuits, such as those that cover slack appearing at the end of the input circuit, may have a depth that exceeds that of the original circuit, as the SI tuning circuit will have a depth twice that of the subcircuit slice leading up to the slack window (as seen in Fig. 6). Although past work [24] that leverages reversibility does not take circuit depth increase into consideration, not doing so could potentially push beyond the frontier of the targeted device. This is intuitive because with noisy quantum devices, we are likely to be executing applications that are already at the brink of a quantum machine’s capability i.e. at the machine’s critical circuit depth. Building tuning circuits beyond this critical depth can be detrimental to optimizing the original circuit.

Thus, to be mindful of the limitations of near-term hardware in terms of gate error and decoherence, TS-SI can be run using the bounds of the depth, or critical path, of the original circuit as criteria it must not violate. This version of TimeStitch is known as Slice-Inverse+Criteria (TS-SI+C).

Note that it is appropriate to focus only on the two-qubit operations along the circuit critical path as a measure of circuit depth. Two-qubit operations dominate in terms of influence on program output because on average, their error rates and duration are $>10x$ of a single-qubit operation [15]. This is particularly favorable for TimeStitch because large slack windows have two-qubit depth that are likely considerably lower than the critical depth (which is a key reason why large slack windows exist). Moreover, large slack windows are likely to provide the most benefits due to the widest space for gate position tuning.

With TS-SI+C, depth is calculated for each of the SI tuning circuits and those of depth less than or equal to the depth of the original circuit are marked for use during TS-SI+C slack window gate position tuning. All untuned slack windows maintain default ALAP scheduling. Examples of circuit locations eligible and ineligible for TS-SI and TS-SI+C tuning for TimeStitch optimization are pictured in Fig. 7. In the original compiled circuit used as TimeStitch input, slack windows 1, 2, and 3 are eligible for TS-SI as they all have tunable single-qubit operations. However, only slack windows 1 and 2 satisfy the depth criteria and are thus tuned by TS-SI+C. Note that there are many other locations in the circuit, such as slack windows without single-qubit gates or periods before qubit runtime begins, that are ineligible for slack tuning entirely.

V. METHODOLOGY

A. Evaluation Effort: Quantities / Constraints

We perform all our experiments on actual IBM quantum machines to faithfully capture true device characteristics. There will be a severe scarcity in the near-term of the availability of quantum resources in the cloud as demand is ever growing.

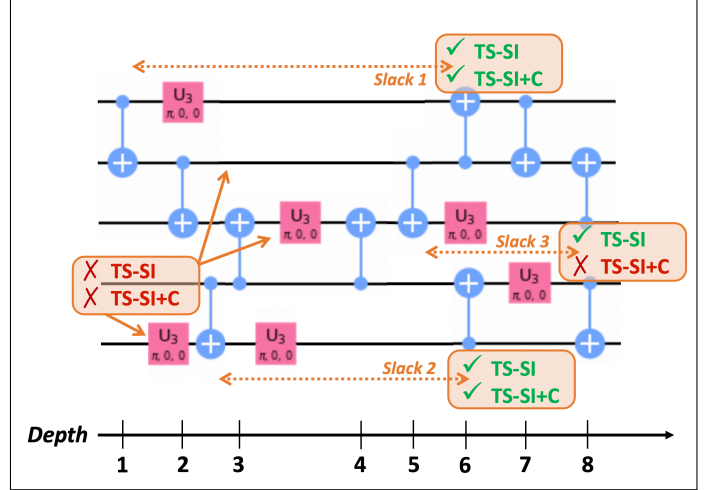


Fig. 7: Example of eligible and ineligible circuit locations for TS-SI and TS-SI+C tuning. Here, slack windows 1, 2, and 3 are eligible for TS-SI as they all have tunable single-qubit operations. However, only slack windows 1 and 2 satisfy the depth criteria and are thus tuned by TS-SI+C.

A first-order impact of quantum machine scarcity are the long queuing times experienced while accessing cloud machines.

This severely impacts the availability of target machines for consistent and disciplined evaluation over long periods of time, which is important due to the spatial and temporal variability in machine noise characteristics.

For this work, we have performed machine executions over nearly a 12 month period, with tests runs on over 20 different quantum machines for over 20 applications. Our evaluations encompass roughly 2,500 quantum jobs to the cloud, comprising of over 600,000 circuits, with confidence built on a total of over 4,000,000,000 machine trials / executions. Out of these, we show results for 11 applications, each paired to a target machine satisfying the following criteria: a) consistent machine availability, b) non-negligible probability ($>10\%$) of the correct application output of (note: this restricts the sizes of applications, as is expected in the near-term), c) limited variability in correct output probabilities and d) maximizing machine qubit utilization (i.e. number of machine qubits closer to number of application qubits) while respecting the previous constraints.

B. Circuits for Evaluation

The framework is evaluated on benchmarks representative of real-world use cases, which are described below and listed in Table I.

Quantum Fourier Transform: QFT is a circuit used as a building block for applications such as Shor’s factoring and phase estimation. It converts a quantum state from the computational basis to the Fourier basis through the introduction of phase. QFT was constructed for 3, 4 and 5 qubits [23].

Quantum Approximate Optimization Algorithm: QAOA [10] is a variational quantum-classical algorithm that can be trained to output bitstrings to solve combinatorial optimization problems. QAOA is implemented atop a parameterized circuit called an ansatz and we use one instance of a hardware efficient QAOA ansatz as the benchmark. We use QAOA ansatz constructed for 4 and 6 qubits.

Variational Quantum Eigensolver: VQE [25] is another hybrid algorithm like QAOA. The goal of this algorithm is to variationally find the lowest eigenvalue of a given problem matrix. We implement VQE on a hardware-efficient SU2 ansatz [2] and use one instance as the benchmark. We construct the ansatz for 4 qubits (4 reps / full entanglement) and 6 qubits (3 / SCA).

Gibbs State Prep: The preparation of quantum Gibbs state has wide-ranging applications in quantum simulation, optimization, and machine learning. We take a VarQITE ansatz based approach to creating the Gibbs state [42] and use one instance as the benchmark. We use 5 qubits. Note: Gibbs is a state preparation circuit with known outputs, meaning that it is a practical usecase for the “Ground Truth” approach.

Quantum Repetition Code Encoder: Error correcting codes are the means by which fault-tolerant quantum computers are able to execute arbitrarily long programs. Here we target a repetition code encoder whose effect is to distribute the quantum information in the initial state across an entangled N-party logical state. This introduces redundancy to the encoding that can be exploited for error detection [31]. We use an encoder targeting 5 qubits.

Greenberger–Horne–Zeilinger State Prep: GHZ state [13] generation is useful as many complex quantum algorithms begin by entangling all qubits before computation in a state preparation process. GHZ was implemented for 5 qubits. Note: similar to Gibbs, GHZ is a practical usecase for the “Ground-Truth” approach.

Ripple Carry Adder: Adders are a critical logic building block for classical and quantum logic alike. We implemented a linear-depth, 2 bit ripple-carry adder quantum circuit that uses 6 qubits based on the structure described in [7].

C. Infrastructure

In this study, TimeStitch is implemented as a compilation pass that performs schedule optimization on top of a highest-baseline compilation of Qiskit Terra 0.16.4 to map and optimize for the IBM machines [4]. To implement state-of-the-art scheduling, the crosstalk scheduling pass of [22] was also implemented as part of the baseline compile. It is included as an optimization pass in Qiskit.

Our applications are distributed across 5 quantum devices: Guadalupe (16q), Toronto (27q), Rome (5q), Bogota (5q) and Casablanca (7q). Machine details can be found on the IBM Quantum Systems page [3].

A single quantum job of our target quantum machines can execute a batch of up to 900 circuits back-to-back. Thus, we use utilize this entire batch across the tuning of gate positions for different slack windows. Each slack window gets

Bench	Q	D	Key / Out	# SW (/Cons.)	Avg.SW (1e-6 s)	Device
QFT	3	14	101	9 / 3	2.73	Guad.
QFT	4	29	1010	15 / 8	18.89	Toro.
QAOA	4	15	0101 + 1010	10 / 5	8.59	Guad.
VQE	4	54	0111	26 / 14	44.38	Rome
Gibbs	4	6	0000+0101+ 1010+1111	4 / 3	7.08	Rome
QFT	5	46	00101	27 / 9	37.13	Bogota
QEC	5	21	00000 + 01011	6 / 4	11.78	Rome
GHZ	5	8	10101	3 / 3	6.58	Rome
QAOA	6	30	101000 + 111101	8 / 5	25.08	Cas.
VQE	6	40	111111	21 / 11	28.68	Guad.
Adder	6	55	000110 (1+0)	16 / 6	20.57	Guad.

TABLE I: Benchmarks and their characteristics. Q: Number of application qubits, D: Circuit depth in CXs, Key / Out: Application outputs, # SW: Number of windows and those targeted under constraint, Avg.SW: Average window size, Device: Target machine

$N = \frac{900}{\# SW}$ circuit slots for tuning, and the resolution of each window’s gate position sweep is $R = \frac{N}{SW_{length}}$.

The benefits of our proposal on these circuits is evaluated on the *Probability of Success (POS)* metric which is the ratio of a number of error-free trials to the total number of trials - a commonly used metric for evaluating the quality of quantum optimization.

D. Evaluation Comparisons

① *As Late As Possible (ALAP):* ALAP scheduling is the default scheduling technique implemented in the Qiskit compiler and was described in Section I.

② *As Soon As Possible (ASAP):* ASAP scheduling forces all gates appearing in slack windows to be executed at the beginning, immediately after the two-qubit gate that acts as the slack beginning boundary.

③ *Middle:* Middle scheduling is a naive scheduling technique that executes all single qubits within slack at the center of their respective slack windows.

④ *TimeStitch with Circuit Slice and Inverse Tuning (TS-SI):* Corresponds to the design from Section IV-C. This is the first of the two practical approaches, but is unconstrained in terms of circuit depth, thus limited in suitability to only low-depth circuits.

⑤ *TimeStitch with Circuit Slice and Inverse Tuning, plus Criteria (TS-SI+C):* Corresponds to the design from Section IV-D. This practical approach is constrained by the depth of the original circuit, thus applicable to all applications targeted in the near-term and beyond.

⑥ *TimeStitch with Known Ground Truths (TS-GT):* Corresponds to the design from Section IV-B. This is primarily a validation approach except in the case of State Preparation circuits.

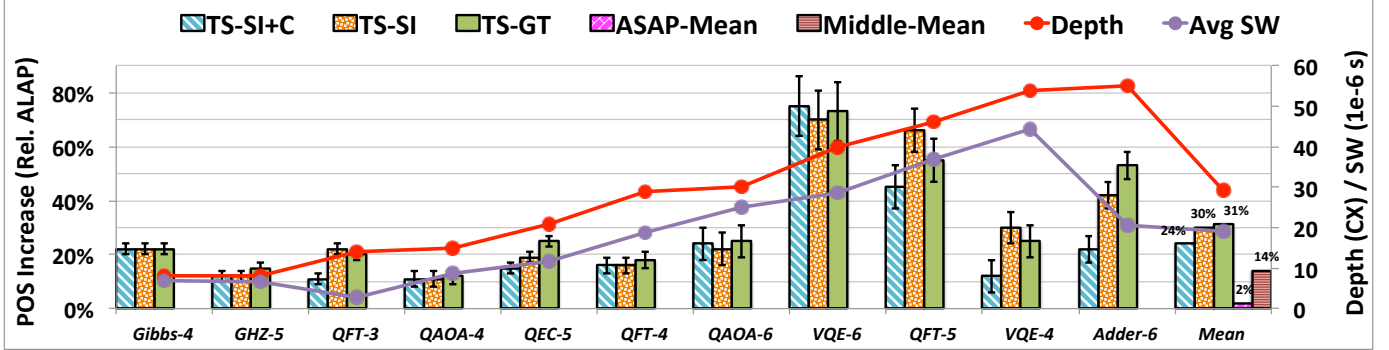


Fig. 8: Comparing the POS benefits of different TS approaches over the ALAP baseline. Mean benefits of ASAP and Middle are also shown. GT benefits are highest, as it is the ideal approach, but is closely followed by TS-SI showing the effectiveness of the SI approach. TS-SI+C provides lower benefits but is still a 24% improvement of the baseline capturing a larger fraction of the ideal benefits.

VI. EVALUATION

A. Probability of Success

In Fig. 8 we show benefits for TimeStitch relative to the ALAP baseline. Benefits shown are in terms of the increase in POS (i.e. fidelity). For TimeStitch, we show results for the 3 versions: TS-SI+C, TS-SI and TS-GT. We also show mean comparisons to ASAP and Middle. These are explained in Section V-D. Applications are ordered by their circuit depth (i.e. number of CX s in the circuit critical path)

On average, TS-GT achieves a 31% POS improvement over ALAP. Of specific interest to TS-GT are the State Preparation circuits which show POS improvements of 22% and 15% respectively. These circuits are directly suited to the TS-GT approach. TS-SI matches TS-GT closely, achieving a mean 30% POS improvement, clearly showing the efficiency of the Slice and Inverse technique in meeting the ideal improvement target. TS-SI+C constrains the Slice and Inverse technique, so that no SI tuning circuit exceeds the gate depth of the original circuit. Even with this constraint, a mean 24% improvement is obtained, indicating that even under constraint, multiple critical slack windows can be tuned for significant benefits. In comparison, ASAP performs similar to ALAP, while Middle achieves a moderate 14% POS improvement. These highlight the benefits of tuning single-qubit gates within slack windows, especially with practical TimeStitch approaches.

Over the three TS techniques, per-application improvements vary from 11% to 75%, depending on the number of slack windows, the size of the slack windows, the criticality of the slack window, impact of the specific gate error on application fidelity, the input state vectors, as well as general noise characteristics of the machine. Table. I provides details on slack windows in the compiled circuits among other details. In Fig. 8, we also plot the depth of the circuit in CX s and the average size of the slack window for each application. It is clear that benefits increase with greater circuit depth. This can be attributed to two reasons: a) the sizes of the slack windows increase with deeper circuits (this is evident from the average slack window size trend matching the circuit depth trend) and

thus provides more room for gate position tuning, and b) POS is lower for deeper circuits, meaning that the impact of tuning benefits are more significant. This is especially important since it is critical in the near-term to improve the execution of quantum applications with less than acceptable circuit fidelity.

Note that we add error bars to the graphs to indicate variation in relative POS benefits from a 1% change to the application’s POS. For applications with lower baseline fidelity (10-15%) like QFT-5 and VQE-6, these error bars are longer, but POS benefits are considerable irrespective. But some variation is expected across runs, which also indicates why TS-SI+C might outperform TS-SI / TS-GT on occasion depending on the particular run’s machine characteristics and calibration.

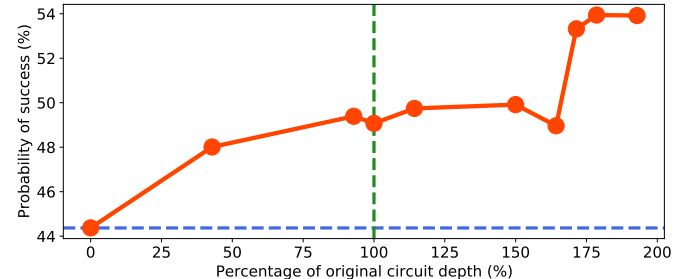


Fig. 9: Threshold sensitivity of window tuning for QFT-3. The blue line represents the ALAP POS, the green line indicates the circuit depth criteria used for TS-SI+C, and the red line describes change in POS as the number of SI tuned slack windows increases.

B. Depth Threshold Sensitivity

In Section IV-D we motivated the need for restricting the SI tuning circuit depth to the depth of the original circuit. Here, we sweep through varying limiting thresholds for the depth of the SI circuit from 0 (i.e. no tunable slack windows) to 2x the original circuit depth (i.e. all 9 slack windows are tunable, equivalent to the unconstrained approach in Section IV-C).

Fig. 9 shows the POS for the QFT-3 circuit for these different thresholds. The baseline ALAP POS (blue line) as well as the depth of the original circuit (green line) are also shown. It is evident that 3 of the 9 windows and SI circuits satisfy the depth criteria.

Adjusting the target depth threshold of slack tuning can influence the POS. For example, if criteria is fixed such that tuning circuit depth must not surpass 50% of the original circuit depth, the POS of rescheduled QFT-3 is around 48%. If machine robustness allowed an increase in criteria bounds to 175% the depth of the original circuit, POS jumps to 53%. Depth thresholds can be set based on the machine-application fit.

Note that the experimental results suffer from some variation effects of the real machine hence we do not see a strictly monotonically increasing curve.

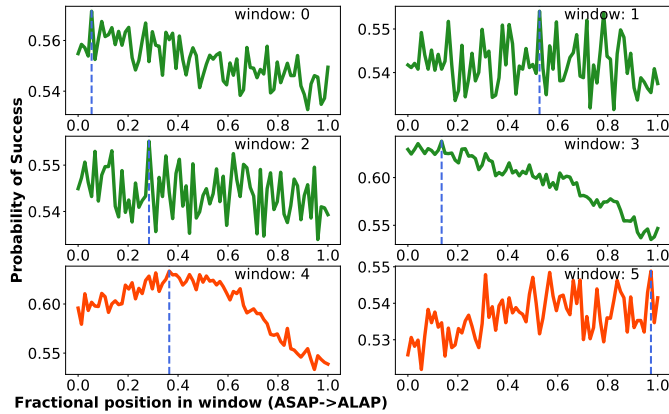


Fig. 10: Slack windows of QEC-5, showing range of POS achieved by tuning each window. Green windows are selected under TS-SI+C while red are rejected.

C. Comparing Slack Windows

In Fig. 10 we show the slack windows of the QEC-5 application, and the change in POS as gate positions are varied from ASAP (left) to ALAP (right). The windows that are suited to the depth constraint imposed by TS-SI+C are shown in green while the others are in red. First, it is clear that there are non-negligible POS variations in 4 out of the 6 windows and all windows have different optimal gate positions. Second, among the green windows, there is considerable benefit in moving to ASAP for window 3. Third, among the red windows, there is considerable benefit for window 4 near the middle of the window. Thus, benefits of TS-SI+C are considerable over the ALAP baseline and under relaxed constraints TS-SI can produce even greater benefits. Similar trends exists across other applications.

D. Comparison against Dynamic Decoupling

Dephasing error compounds during runtime and plagues quantum circuits. DD has shown to be effective on a small scale for correcting single qubit states and, to a lesser extent, two-qubit entangled states in superconducting systems [26] at

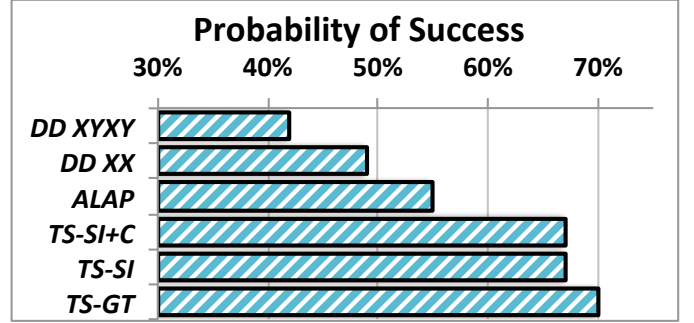


Fig. 11: Comparison of POS between DD, ALAP, and Timestitch for GHZ benchmark on IBM Q Rome.

the cost of additional circuit instructions. Single-qubit gate errors are on average of order 10^{-4} [1], [15]. Although small, collective noise can degrade circuit performance, especially as circuits scale. Limiting depth is critical, and we attempt to respect the machine coherence constraints with depth criteria in TS-SI+C, described in Section IV-D.

Naive insertion of additional instructions can extend runtime, pushing circuit depth past to the device’s thresholds. The negative impacts of additional circuit instructions produced by standard implementations of DD that insert refocusing sequences after all circuit instructions are shown in Fig. 11. Here, the probability of success (POS) for a five-qubit GHZ benchmark is reported for six different implementations. The first two implementations include standard DD correction using XX and XYXY sequences [39], but the corrective benefits of DD do not outweigh the impact of the additional instructions adding gate error and runtime. DD performs significantly worse than the default ALAP compilation. The best GHZ schedule in Fig. 11 is produced by TS-GT followed by TS-SI and TS-SI+C.

VII. RELATED WORK

Related Quantum Proposals: Past work includes the development of methodologies that impact decoherence in quantum circuits by reducing depth and thus overall circuit runtime [6], [18], [19], [33], [38], [43]. These works, however, although targeted to real QC topologies, do not consider variational QC characteristics such as gate error rates and gate durations for their techniques. There also exist frameworks that aim to decrease quantum circuit noise by taking device calibration data into consideration to improve program success [21], [34], [40], but these techniques do not implement optimizations that take advantage of slack time in circuits. Next, optimizing schedulers exist that mitigate noise associated with crosstalk by considering device properties [8], [22]. Finally, the methods of [41] takes advantage of quantum circuit slack, but the technique focuses on the qubit mapping problem rather than error reduction on real quantum machines. Further, the benefits of our method complement other indirect decoherence mitigation approaches [17], [21].

Exploiting Slack in Classical Computing: With the critical need for maximizing performance under strict power budgets in the classical world, exploiting any form of idle time or slack in classical computing has been a popular theme of research over past decades. At the circuit level, slack (in a clock cycle) can stem from the favorable effects of process, voltage, temperature, as well as data based variations in the presence of conservative timing guardbands. These have been exploited with multiple better-than-worse-case approaches [9], [14], [28]–[30], [36]. Similarly, at the micro-architecture level, periods of time with less or no-activity can help save power at no additional performance costs. These are often exploited via power/clock gating, multi threading [37], instruction rescheduling [11] and so on.

VIII. CONCLUSION

Reducing the impact of quantum errors is critical for substantial advancements in the near term that will allow the achievement of fault-tolerance. The unintentional coupling of qubits to their environment, and each other, adds significant noise to computation, and improved methods to combat decoherence are required to boost the performance of quantum algorithms on real machines. Here, slack tuning improves the fidelity of compiled quantum circuits without either increasing total gate count or introducing circuit partitioning that increases circuit runtime. By exploiting circuit reversibility and by constraining tuning circuits to the depth of the original application, we propose a practical design suited to all applications and quantum machines, especially applications which run at the lower limits of fidelity requirements which are critical to improve.

This paper presents a novel technique that takes advantage of a previously unexplored space of quantum circuit slack, opening up a new domain of exploration. In future work, we hope to investigate more slack based optimization directions such as those targeting applications with known information about the outcomes, including specialized state preparation circuits, variational quantum algorithms etc. Moreover, modeling these newly explored machine characteristics into simulators can accelerate some of these research directions.

REFERENCES

- [1] “IBM Quantum Experience,” <https://quantum-computing.ibm.com>, accessed: 2020-11-18.
- [2] “Ibm quantum su2 ansatz,” <https://qiskit.org/documentation/stubs/qiskit.circuit.library.EfficientSU2.html>, accessed: 2020-11-18.
- [3] “IBM quantum systems,” <https://quantum-computing.ibm.com/services?systems=all>, accessed: 2020-11-18.
- [4] H. Abraham, AduOffei, R. Agarwal, I. Y. Akhalwaya, G. Aleksandrowicz, T. Alexander, M. Amy, E. Arbel, Arjit02, A. Asfaw, A. Avkhadiev, C. Azaustre, AzizNgoueya, A. Banerjee, A. Bansal, P. Barkoutsos, G. Barron, G. S. Barron, L. Bello, Y. Ben-Haim, D. Bevenius, A. Bhobe, L. S. Bishop, C. Blank, S. Bolos, S. Bosch, Brandon, S. Bravyi, Bryce-Fuller, D. Bucher, A. Burov, F. Cabrera, P. Calpin, L. Capelluto, J. Carballo, G. Carrascal, A. Chen, C.-F. Chen, E. Chen, J. C. Chen, R. Chen, J. M. Chow, S. Churchill, C. Claus, C. Clauss, R. Cocking, F. Correa, A. J. Cross, A. W. Cross, S. Cross, J. Cruz-Benito, C. Culver, A. D. Córcoles-Gonzales, S. Dague, T. E. Dandachi, M. Daniels, M. Dartailh, DavideFrr, A. R. Davila, A. Dekusar, D. Ding, J. Doi, E. Drechsler, Drew, E. Dumitrescu, K. Dumon, I. Duran, K. EL-Safty, E. Eastman, G. Eberle, P. Eendebak, D. Egger, M. Everitt, P. M. Fernández, A. H. Ferrera, R. Foulland, FranckChevallier, A. Frisch, A. Fuhrer, B. Fuller, M. GEORGE, J. Gacon, B. G. Gago, C. Gambella, J. M. Gambetta, A. Gammanpila, L. Garcia, T. Garg, S. Garion, A. Gilliam, A. Giridharan, J. Gomez-Mosquera, S. de la Puente González, J. Gorzinski, I. Gould, D. Greenberg, D. Grinko, W. Guan, J. A. Gunnels, M. Haglund, I. Haide, I. Hamamura, O. C. Hamido, F. Harkins, V. Havlicek, J. Hellmers, Ł. Herok, S. Hillmich, H. Horii, C. Howington, S. Hu, W. Hu, J. Huang, R. Huisman, H. Imai, T. Imamichi, K. Ishizaki, R. Iten, T. Itoko, JamesSeaward, A. Javadi-Abhari, Jessica, M. Jivrajani, K. Johns, S. Johnstun, Jonathan-Shoemaker, V. K. T. Kachmann, N. Kanazawa, Kang-Bae, A. Karazeev, P. Kassebaum, J. Kelso, S. King, Knabberjoe, Y. Kobayashi, A. Kovyrshin, R. Krishnakumar, V. Krishnan, K. Krsulich, P. Kumkar, G. Kus, R. LaRose, E. Lacal, R. Lambert, J. Lapeyre, J. Latone, S. Lawrence, C. Lee, G. Li, D. Liu, P. Liu, Y. Maeng, K. Majmudar, A. Malyshев, J. Manela, J. Marecek, M. Marques, D. Maslov, D. Mathews, A. Matsuo, D. T. McClure, C. McGarry, D. McKay, D. McPherson, S. Meesala, T. Metcalfe, M. Mevissen, A. Meyer, A. Mezzacapo, R. Midha, Z. Minev, A. Mitchell, N. Moll, J. Montanez, M. D. Mooring, R. Morales, N. Moran, M. Motta, P. Murali, J. Müggenburg, D. Nadlinger, K. Nakanishi, G. Nannicini, P. Nation, E. Navarro, Y. Naveh, S. W. Neagle, P. Neuweiler, J. Nicander, P. Niroula, H. Norlen, NuoWenLei, L. J. O’Riordan, O. Ogunbayo, P. Ollitrault, R. Otaolea, S. Oud, D. Padilha, H. Paik, S. Pal, Y. Pang, S. Perriello, A. Phan, F. Piro, M. Pistoia, C. Piveteau, P. Pocreau, A. Pozas-iKerstjens, V. Prutyanov, D. Puzzuoli, J. Pérez, Quintii, R. I. Rahman, A. Raja, N. Ramagiri, A. Rao, R. Raymond, R. M.-C. Redondo, M. Reuter, J. Rice, M. L. Rocca, D. M. Rodríguez, RohithKarur, M. Rossmannek, M. Ryu, T. SAPV, SamFerracin, M. Sandberg, H. Sandesara, R. Sapra, H. Sargsyan, A. Sarkar, N. Sathaye, B. Schmitt, C. Schnabel, Z. Schoenfeld, T. L. Scholten, E. Schoute, J. Schwarm, I. F. Sertage, K. Setia, N. Shammah, Y. Shi, A. Silva, A. Simonetto, N. Singstock, Y. Siraichi, I. Sitzdikov, S. Sivarajah, M. B. Sletfjerding, J. A. Smolin, M. Soeken, I. O. Sokolov, I. Sokolov, SooluThomas, Starfish, D. Steenken, M. Stypulkoski, S. Sun, K. J. Sung, H. Takahashi, T. Takawale, I. Tavernelli, C. Taylor, P. Taylor, S. Thomas, M. Tillet, M. Tod, M. Tomasik, E. de la Torre, K. Trabing, M. Treinish, TrishaPe, D. Tulsi, W. Turner, Y. Vaknin, C. R. Valcarce, F. Varhon, A. C. Vazquez, V. Villar, D. Vogt-Lee, C. Vuillot, J. Weaver, J. Weidenfeller, R. Wieczorek, J. A. Wildstrom, E. Winston, J. J. Woehr, S. Woerner, R. Woo, C. J. Wood, R. Wood, S. Wood, S. Wood, J. Wootton, D. Yeralin, D. Yonge-Mallo, R. Young, J. Yu, C. Zachow, L. Zdanski, H. Zhang, and C. Zoufal, “Qiskit: An open-source framework for quantum computing,” 2019.
- [5] J. Biamonte, P. Wittek, N. Pancotti, P. Rebentrost, N. Wiebe, and S. Lloyd, “Quantum machine learning,” *Nature*, vol. 549, no. 7671, pp. 195–202, 2017.
- [6] A. M. Childs, E. Schoute, and C. M. Unsal, “Circuit transformations for quantum architectures,” *arXiv preprint arXiv:1902.09102*, 2019.
- [7] S. A. Cuccaro, T. G. Draper, S. A. Kutin, and D. P. Moulton, “A new quantum ripple-carry addition circuit,” *arXiv preprint quant-ph/0410184*, 2004.
- [8] Y. Ding, P. Gokhale, S. F. Lin, R. Rines, T. Propson, and F. T. Chong, “Systematic crosstalk mitigation for superconducting qubits via frequency-aware compilation,” *arXiv preprint arXiv:2008.09503*, 2020.
- [9] D. Ernst, Nam Sung Kim, S. Das, S. Pant, R. Rao, Toan Pham, C. Ziesler, D. Blaauw, T. Austin, K. Flautner, and T. Mudge, “Razor: a low-power pipeline based on circuit-level timing speculation,” in *Proceedings. 36th Annual IEEE/ACM International Symposium on Microarchitecture, 2003. MICRO-36.*, 2003, pp. 7–18.
- [10] E. Farhi, J. Goldstone, and S. Gutmann, “A quantum approximate optimization algorithm,” *arXiv preprint arXiv:1411.4028*, 2014.
- [11] B. Fields, R. Bodík, and M. D. Hill, “Slack: Maximizing performance under technological constraints,” in *Proceedings of the 29th Annual International Symposium on Computer Architecture*, ser. ISCA ’02. USA: IEEE Computer Society, 2002, p. 47–58.
- [12] T. Giurgica-Tiron, Y. Hindy, R. LaRose, A. Mari, and W. J. Zeng, “Digital zero noise extrapolation for quantum error mitigation,” in *2020 IEEE International Conference on Quantum Computing and Engineering (QCE)*. IEEE, 2020, pp. 306–316.
- [13] D. M. Greenberger, M. A. Horne, and A. Zeilinger, “Going beyond bell’s theorem,” in *Bell’s theorem, quantum theory and conceptions of the universe*. Springer, 1989, pp. 69–72.
- [14] M. Gupta, J. A. Rivers, P. Bose, G.-Y. Wei, and D. Brooks, “Tribeca: De-

sign for pvt variations with local recovery and fine-grained adaptation,” in *MICRO*, 2009.

[15] P. Jurcevic, A. Javadi-Abhari, L. S. Bishop, I. Lauer, D. Borgorin, M. Brink, L. Capelluto, O. Gunluk, T. Itoko, N. Kanazawa *et al.*, “Demonstration of quantum volume 64 on a superconducting quantum computing system,” *Quantum Science and Technology*, 2021.

[16] A. Kandala, A. Mezzacapo, K. Temme, M. Takita, M. Brink, J. M. Chow, and J. M. Gambetta, “Hardware-efficient variational quantum eigensolver for small molecules and quantum magnets,” *Nature*, vol. 549, no. 7671, pp. 242–246, 2017.

[17] G. Li, Y. Ding, and Y. Xie, “Tackling the qubit mapping problem for nisq-era quantum devices,” in *Proceedings of the Twenty-Fourth International Conference on Architectural Support for Programming Languages and Operating Systems*, 2019, pp. 1001–1014.

[18] D. Maslov, S. M. Falconer, and M. Mosca, “Quantum circuit placement,” *IEEE Transactions on Computer-Aided Design of Integrated Circuits and Systems*, vol. 27, no. 4, pp. 752–763, 2008.

[19] T. S. Metodi, D. D. Thaker, A. W. Cross, F. T. Chong, and I. L. Chuang, “Scheduling physical operations in a quantum information processor,” in *Quantum Information and Computation IV*, vol. 6244. International Society for Optics and Photonics, 2006, p. 62440T.

[20] N. Moll, P. Barkoutsos, L. S. Bishop, J. M. Chow, A. Cross, D. J. Egger, S. Filipp, A. Fuhrer, J. M. Gambetta, M. Ganzhorn *et al.*, “Quantum optimization using variational algorithms on near-term quantum devices,” *Quantum Science and Technology*, vol. 3, no. 3, p. 030503, 2018.

[21] P. Murali, J. M. Baker, A. Javadi-Abhari, F. T. Chong, and M. Martonosi, “Noise-adaptive compiler mappings for noisy intermediate-scale quantum computers,” in *Proceedings of the Twenty-Fourth International Conference on Architectural Support for Programming Languages and Operating Systems*, 2019, pp. 1015–1029.

[22] P. Murali, D. C. McKay, M. Martonosi, and A. Javadi-Abhari, “Software mitigation of crosstalk on noisy intermediate-scale quantum computers,” in *Proceedings of the Twenty-Fifth International Conference on Architectural Support for Programming Languages and Operating Systems*, 2020, pp. 1001–1016.

[23] M. A. Nielsen and I. Chuang, *Quantum computation and quantum information*. Cambridge University Press, 2010.

[24] T. Patel and D. Tiwari, “Qraft: reverse your quantum circuit and know the correct program output,” *Proceedings of the 26th ACM International Conference on Architectural Support for Programming Languages and Operating Systems*, 2021.

[25] A. Peruzzo, J. McClean, P. Shadbolt, M.-H. Yung, X.-Q. Zhou, P. J. Love, A. Aspuru-Guzik, and J. L. O’Brien, “A variational eigenvalue solver on a photonic quantum processor,” *Nature communications*, vol. 5, no. 1, pp. 1–7, 2014.

[26] B. Pokharel, N. Anand, B. Fortman, and D. A. Lidar, “Demonstration of fidelity improvement using dynamical decoupling with superconducting qubits,” *Physical review letters*, vol. 121, no. 22, p. 220502, 2018.

[27] J. Preskill, “Quantum computing in the nisq era and beyond,” *Quantum*, vol. 2, p. 79, 2018.

[28] G. S. Ravi and M. Lipasti, “Recycling data slack in out-of-order cores,” in *2019 IEEE International Symposium on High Performance Computer Architecture (HPCA)*, 2019, pp. 545–557.

[29] G. S. Ravi, *Integrating Computing Systems from the Gates Up: Breaking the Clock Abstraction*. The University of Wisconsin-Madison, 2020.

[30] G. S. Ravi and M. Lipasti, “Aggressive slack recycling via transparent pipelines,” *Proceedings of the International Symposium on Low Power Electronics and Design*, 2018.

[31] J. Roffe, “Quantum error correction: an introductory guide,” *Contemporary Physics*, vol. 60, no. 3, p. 226–245, Jul 2019. [Online]. Available: <http://dx.doi.org/10.1080/00107514.2019.1667078>

[32] P. W. Shor, “Polynomial-time algorithms for prime factorization and discrete logarithms on a quantum computer,” *SIAM review*, vol. 41, no. 2, pp. 303–332, 1999.

[33] M. Y. Siraichi, V. F. d. Santos, S. Collange, and F. M. Q. Pereira, “Qubit allocation,” in *Proceedings of the 2018 International Symposium on Code Generation and Optimization*, 2018, pp. 113–125.

[34] S. S. Tannu and M. K. Qureshi, “Not all qubits are created equal: A case for variability-aware policies for nisq-era quantum computers,” in *Proceedings of the Twenty-Fourth International Conference on Architectural Support for Programming Languages and Operating Systems*, ser. ASPLOS ’19. New York, NY, USA: Association for Computing Machinery, 2019, p. 987–999. [Online]. Available: <https://doi.org/10.1145/3297858.3304007>

[35] K. Temme, S. Bravyi, and J. M. Gambetta, “Error mitigation for short-depth quantum circuits,” *Physical review letters*, vol. 119, no. 18, p. 180509, 2017.

[36] A. Tiwari, S. R. Sarangi, and J. Torrellas, “Recycle:: Pipeline adaptation to tolerate process variation,” in *ISCA ’07*, 2007, pp. 323–334.

[37] D. M. Tullsen, S. J. Eggers, and H. M. Levy, “Simultaneous multithreading: Maximizing on-chip parallelism,” in *Proceedings of the 22nd Annual International Symposium on Computer Architecture*, ser. ISCA ’95. New York, NY, USA: Association for Computing Machinery, 1995, p. 392–403. [Online]. Available: <https://doi.org/10.1145/223982.224449>

[38] D. Venturelli, M. Do, E. Rieffel, and J. Frank, “Compiling quantum circuits to realistic hardware architectures using temporal planners,” *Quantum Science and Technology*, vol. 3, no. 2, p. 025004, 2018.

[39] L. Viola, E. Knill, and S. Lloyd, “Dynamical decoupling of open quantum systems,” *Physical Review Letters*, vol. 82, no. 12, p. 2417, 1999.

[40] C. Vuillot, “Is error detection helpful on ibm 5q chips?” *arXiv preprint arXiv:1705.08957*, 2017.

[41] C. Zhang, Y. Chen, Y. Jin, W. Ahn, Y. Zhang, and E. Z. Zhang, “Slackq: Approaching the qubit mapping problem with a slack-aware swap insertion scheme,” *arXiv preprint arXiv:2009.02346*, 2020.

[42] C. Zoufal, A. Lucchi, and S. Woerner, “Variational quantum boltzmann machines,” *Quantum Machine Intelligence*, vol. 3, no. 1, Feb 2021. [Online]. Available: <http://dx.doi.org/10.1007/s42484-020-00033-7>

[43] A. Zulehner and R. Wille, “Compiling su (4) quantum circuits to ibm qx architectures,” in *Proceedings of the 24th Asia and South Pacific Design Automation Conference*, 2019, pp. 185–190.